

# Herb-Drug interactions between Aidi injection and doxorubicin in rats with diethylnitrosamine-induced hepatocellular carcinoma

**Yuan Lu**

Guizhou Medical University <https://orcid.org/0000-0002-0045-2483>

**Jie Pan**

Guizhou Medical University

**Shuai Zhang**

Guizhou Medical University

**Liu Chunhua**

Guizhou Medical University

**Jia Sun**

Guizhou Medical University

**Yueting Li**

Guizhou Medical University

**Siyang Chen**

Guizhou Medical University

**Jing Huang**

Guizhou Medical University

**Chuang Cao**

Guizhou Medical University

**Yonglin Wang**

Guizhou Medical University

**Yongjun Li**

Guizhou Medical University

**Ting Liu (✉ [t-liu@163.com](mailto:t-liu@163.com))**

<https://orcid.org/0000-0002-5824-3975>

---

## Research article

**Keywords:** Herb-drug interaction, Hepatocellular carcinoma, Aidi Injection, Doxorubicin, Doxorubicinol

**Posted Date:** June 3rd, 2020

**DOI:** <https://doi.org/10.21203/rs.3.rs-27460/v1>

**License:**  This work is licensed under a Creative Commons Attribution 4.0 International License.

[Read Full License](#)

---

# Abstract

## Background

Aidi Injection (ADI), a Chinese herbal preparation with anti-cancer activity, is used for the treatment of hepatocellular carcinoma (HCC). Several clinical studies have shown that co-administration of ADI with doxorubicin (DOX) is associated with reduced toxicity of chemotherapy, enhanced clinical efficacy and improved quality of life for patients. However, limited information is available about the herb-drug interactions between ADI and DOX. The study aimed to investigate the pharmacokinetic mechanism of herb-drug interactions between ADI and DOX in a rat model of HCC.

## Methods

Experimental HCC was induced in rats by oral administration of diethylnitrosamine. The HCC rats were pretreated with ADI (10 mL/kg, intraperitoneal injection) for 14 consecutive days prior to administration of DOX (7 mg/kg, intravenous injection) to investigate pharmacokinetic interactions. Plasma concentrations of DOX and its major metabolite, doxorubicinol (DOXol), were determined using ultra-performance liquid chromatography-tandem mass spectrometry (UPLC-MS/MS).

## Results

Preadministration of ADI significantly altered the pharmacokinetics of DOX in HCC rats, leading to increased plasma concentrations of both DOX and DOXol. The plasma drug concentration-time curves (AUCs) of DOX and DOXol in rats pretreated with ADI were 3.79-fold and 2.92-fold higher, respectively, than those in control rats that did not receive ADI.

## Conclusions

Increased levels of DOX were found in the plasma of HCC rats pretreated with ADI, which may lead to enhanced efficacy but also potential toxicity.

### 1. Background

Hepatocellular carcinoma (HCC) is one of the most common liver malignancies in regions where chronic hepatitis or liver diseases are prevalent, such as China [1]. Doxorubicin (DOX) is a key drug used in chemotherapy of HCC but its clinical utility is limited by both drug resistance and cardiotoxicity [2]. It has previously been suggested that the main active metabolite of DOX, doxorubicinol (DOXol), contributes to both the efficacy and toxicity of DOX [3].

Aidi Injection (ADI), which contains extracts of *Astragalus Radix*, *Acanthopanax senticosus*, *Ginseng Radix* and *Mylibris* is widely used in China for the treatment of HCC. Several clinical studies have shown that combining ADI with chemotherapy reduces the toxicity of chemotherapy, enhances clinical efficacy and improves the quality of life of cancer patients [4–7]. Cantharidin, the major bioactive component of *Cantharis*, has potent antitumor activity, induces apoptosis in a variety of tumor cells, increases numbers of white blood cells and reduces the occurrence of bone marrow suppression [8–11]. Recent pharmacological studies have shown that astragalus polysaccharides have significant immunomodulatory activity [12], are hepatoprotective and antioxidant [13–14], and have antitumor effects [15]. *A. senticosus* also has antitumor and immunomodulatory effects [16]. Ginsenosides, such as ginsenosides Rg<sub>3</sub> and Rh<sub>2</sub>, show antitumor and antiangiogenic effects in various models using tumor cells and vascular endothelial cells [17–18]. These effects are, however, insufficient to explain why ADI improves the clinical efficacy of chemotherapy drugs and the mechanism leading to increased efficacy needs to be explained. Blood concentrations are generally believed to be proportional to the therapeutic effect and toxicity of a drug. Many patients use ADI for HCC, before and after treatment with DOX, to reduce toxicity and improve the efficacy of chemotherapy. So far, there have been no reports describing research into herb-drug interactions between ADI and DOX and the nature of the interaction remains unknown.

There are potential risks in co-administering ADI with DOX in an outpatient setting and a pharmacokinetic study to evaluate potential interactions of ADI with DOX is needed. We hypothesized that ADI may alter the pharmacokinetics of DOX and used rats with experimental HCC to evaluate this hypothesis. HCC rats were pretreated with ADI (10 mL/kg, once a day, by intraperitoneal (i.p.) injection) for 14 consecutive days prior to administration of DOX (7 mg/kg by intravenous (i.v.) injection) to investigate pharmacokinetic interactions.

## 2. Methods

### 2.1. Chemicals and reagents

ADI (Product No. 20150627) was supplied by Guizhou Ebay Pharmaceutical Co., Ltd. (Guizhou, China). Diethylnitrosamine, doxorubicin (25316-40-9), doxorubicinol (54193-28-1), and the internal standard (IS) tropisetron hydrochloride (105826-92-4) were all purchased from Dalian Meilun Biotech Co., Ltd. (Liaoning, China). HPLC-grade acetonitrile, methanol and formic acid was supplied by Merck Company Inc. (Darmstadt, Germany). Distilled water was obtained from Watsons Group Co., Ltd. (Hong Kong, PRC). All chemicals and reagents used were of chromatographic or analytical grade.

### 2.2. Animals

All experimental procedures were conducted according to the Institutional Animal Care guidelines and approved ethically by the Administration Committee of Experimental Animals, Guizhou Province, China. Male, pathogen-free, Sprague-Dawley rats (180–200 g) were purchased from Changsha Tianqing Biological Technology Co., Ltd. (Changsha, China, Certificate No. SCXK2016-0015) and acclimated for at

least one week in their environmentally controlled quarters ( $25\text{ }^{\circ}\text{C} \pm 2\text{ }^{\circ}\text{C}$  and 12/12 light/dark cycle), with free access to standard chow and water.

## 2.3. Induction of HCC in rats by diethylnitrosamine

Experimental HCC was induced by oral administration of diethylnitrosamine (DEN), as previously described [19–20]. In brief, DEN ( $95\text{ }\mu\text{g/mL}$ ) was administered in drinking water for four consecutive weeks, administration was interrupted for 4 weeks, and then resumed for 8 weeks.

## 2.4. Animal treatment

On the last day of DEN administration, twenty-four HCC rats were randomly divided into two groups of 12 animals, a control group and an ADI group. The control group received saline ( $10\text{ mL/kg}$ , i.p.) once a day for 14 consecutive days and the ADI group received ADI ( $10\text{ mL/kg}$ , i.p.) once a day for 14 consecutive days. The rats were allowed free access to standard chow and water during these 14 days. Access to food was then prohibited for 12 h, with continued free access to water. Six rats from each group were then treated with DOX ( $7\text{ mg/kg}$ , i.v.). Blood samples ( $\sim 250\text{ }\mu\text{L}$ ) were collected from the tail vein into heparinized centrifuge tubes 0.033, 0.083, 0.167, 0.25, 0.333, 0.5, 1, 2, 4 and 8 h after DOX administration. Each blood sample was centrifuged for 5 min at  $3306 \times g$  and an aliquot of the supernatant ( $100\text{ }\mu\text{L}$ ) was transferred to a labeled plastic vial and stored at  $-20\text{ }^{\circ}\text{C}$  before analysis. At the end of study, all animals were euthanized by our veterinary staff in the animal care facility by carbon dioxide asphyxiation.

## 2.5. Pharmacokinetic studies

### 2.5.1 UPLC-ESI-MS conditions

Chromatographic conditions were based on preliminary research work carried out in our laboratory [21]. A Waters ACQUITY UPLC system (Waters Corp., Milford, MA, USA), coupled with a Waters TQD Quantum triple-quadrupole mass spectrometer equipped with an electrospray ionization (ESI) source, was used for determination of the chromatographic analytes. Waters MassLynx software v.4.1 was used for acquisition and data processing. Separation and quantification were performed using a BEH  $\text{C}_{18}$  column ( $50\text{ mm} \times 2.1\text{ mm} \times 1.7\text{ }\mu\text{m}$ , Waters, Wexford, Ireland). The column temperature was  $45\text{ }^{\circ}\text{C}$  and the flow rate was  $0.35\text{ mL/min}$ . The eluent was a mixture of mobile phase A (acetonitrile containing 0.1% formic acid) and mobile phase B (water containing 0.1% formic acid), with a gradient program as follows: 0–0.5 min, 10–30% A; 0.5–1.5 min, 30–60% A; 1.5–2.0 min, 60–90% A; 2.0–3.0 min, 90–10% A. The samples were kept at  $25\text{ }^{\circ}\text{C}$  in the sample manager. The injection volume was  $1.0\text{ }\mu\text{L}$  (partial loop with needle overfill mode). A strong needle wash solution (90:10, methanol-water, v/v) and a weak needle wash solution (10:90, acetonitrile-water, v/v) were used. The mass spectrometer was operated in positive ion mode, with optimized parameters set as follows: nitrogen gas flow,  $650\text{ L/h}$ ; capillary voltage,  $3\text{ kV}$ ; ion source temperature,  $120\text{ }^{\circ}\text{C}$ ; desolvation temperature,  $350\text{ }^{\circ}\text{C}$ . Cone voltages were optimized and set at  $20\text{ V}$ ,  $20\text{ V}$ , and  $32\text{ V}$  for DOX, DOXol, and IS, respectively. Quantification was performed using selected or single ion recording mode by monitoring the parent ions ( $m/z\ 544.3$  for DOX,  $m/z\ 546.3$  for DOXol and  $m/z\ 285.3$  for IS).

## 2.5.2. Sample preparation

Samples were thawed to room temperature before analysis. IS solution [50  $\mu$ L, 50 ng/mL IS dissolved in water/acetonitrile (50:60, v/v)] was added to rat plasma (100  $\mu$ L). After vortexing for 5 min, methanol containing 5% formic acid (450  $\mu$ L) was added to precipitate the proteins. After vortexing, mixing and sonication for 5 min, the sample was centrifuged at 13,000  $\times g$  for 10 min. The supernatant was then transferred to another tube and evaporated to dryness under a gentle stream of nitrogen. The residue was dissolved in mobile phase (mobile phase A: mobile phase B, 10/90; 400  $\mu$ L), centrifuged at 13,000  $\times g$  for 10 min, and an aliquot (1  $\mu$ L) of the solution was injected into the UPLC-MS/MS.

## 2.5.3. Pharmacokinetic analysis

Pharmacokinetic parameters were calculated using Drug and Statistic (DAS) pharmacokinetic software version 2.0 (Mathematical Pharmacology Professional Committee of China, Shanghai, China). A two tailed Student's *t*-test was used to determine the significance of differences in pharmacokinetic parameters between the control group and the ADI group.  $P < 0.05$  was considered to be statistically significant.

## 3. Results

### 3.1. Method validation

Plasma concentrations of DOX and DOXol were quantified using a validated UPLC-MS method previously developed in our laboratory [21]. Briefly, the retention times of tropisetron (IS), DOXol and DOX were 1.57, 1.60 and 1.74 min, respectively. The lower limits of quantification (LLOQ) were 100 ng/mL for DOX and 10 ng/mL for DOXol. The mean recoveries of DOX and DOXol were 83.25 – 96.58% and the intra- and inter-day precisions were  $< 10\%$ . DOX and DOXol in the analytical samples were stable for 12 h in the autosampler, for 72 h at  $-20\text{ }^{\circ}\text{C}$  and over three freeze-thaw cycles. Linearity, sensitivity, selectivity, accuracy, intra- and inter-day precision and stability of the method were validated according to the requirements for bioanalytical methods laid out in the Guidance for Industry Bioanalytical Method Validation Document from the American Food and Drug Administration.

### 3.2. Pharmacokinetic study

The effects of ADI on the pharmacokinetics of DOX in HCC rats were examined by administering a single dose of DOX (7 mg/kg, p.o.) to the rats. Pharmacokinetic investigation showed that the plasma concentration-time data for DOX were best fitted to a two-compartment intravenous open model. A one-compartment model was used to describe the pharmacokinetics of DOXol. Plasma concentrations of DOX were found to be significantly higher in the ADI group than in the control group (Fig. 1). The area under the plasma drug concentration-time curve (AUC) of DOX in the ADI group was 3.79-fold higher than that in the control group. The half-life of distribution ( $t_{1/2\alpha}$ ), apparent volume of distribution in the central compartment ( $V_1$ ) in the ADI group were also significantly higher than in the control group ( $P < 0.01$ ).

Meanwhile, compared with the control group, clearance (CL) of DOX in the ADI group was significantly lower ( $P < 0.05$ ). There were no statistically significant differences in elimination half-life ( $t_{1/2\beta}$ ), elimination rate constant of drug from compartment 1 ( $K_{10}$ ), rate constant for movement of drug from compartment 1 to compartment 2 ( $K_{12}$ ) or rate constant for movement of drug from compartment 2 to compartment 1 ( $K_{21}$ ) between the two groups. The AUC of DOXol, the main metabolite of DOX, was 2.92-fold higher in the ADI group than in the control group. The mean residence time ( $MRT_{0-t}$ ), elimination half-life time ( $t_{1/2z}$ ) and peak concentration ( $C_{max}$ ) of DOXol were all significantly increased in the ADI group compared with the control group (2.22-, 2.39- and 3.46-fold, respectively). Pharmacokinetic analysis thus showed that preadministration of ADI significantly altered the pharmacokinetics of DOX in HCC rats, leading to elevation of plasma concentrations of both DOX and DOXol.

## 4. Discussion

Despite improved diagnostic tools for HCC and much better survival rates of patients, the outcomes and prognoses of HCC patients remain poor because of poor liver function and advanced cancer stage. Transcatheter arterial chemoembolization (TACE) is the main treatment for unresectable HCC, and DOX is one of the commonly used drugs in TACE [22–23]. TACE is not, however, ideal as a long-term cure since it often reduces immunity, aggravates the impairment of liver function and reduces life quality of HCC patients. Finding a way to reduce liver injury and improve clinical efficacy and quality of life has thus become a key issue and many patients in Asia are seeking help from traditional herbal medicines.

ADI is composed mainly of *Astragalus*, *A. senticosus*, *Ginseng* and *Cantharis*. ADI, combined with TACE, is now widely used in the treatment of unresectable HCC in China. It has been reported that this combination can, to some extent, enhance the clinical effect, improve overall survival, increase quality of life for patients and reduce adverse events, including leukopenia, gastrointestinal side effects and liver damage [24]. In a previous study, we found that ADI reduced serum levels of alanine aminotransferase (ALT), aspartate aminotransferase (AST), total bilirubin (TBil) and alkaline phosphatase (ALP) in rats with DEN-induced HCC, confirming its protective effect on liver function [21]. The clinical use of ADI is intravenous drip, 50 to 100 ml of ADI for adults, mixed with 0.9% sodium chloride injection or glucose injection, once a day. When combined with radiotherapy and chemotherapy, the course of treatment is synchronized with radiotherapy and chemotherapy. ADI is used for 10 days before and after surgery. For patients with advanced cachexia, ADI is used for 30 days or depending on the condition. According to human and rat dose conversion and the convenience of practical operation, rats were injected intraperitoneally with 10 mL/kg of ADI for 14 consecutive days.

Our results show that plasma concentrations of DOX and DOXol were significantly higher in the ADI group. AUC of DOX and DOXol in the ADI group was 3.79-fold and 2.92-fold higher than that in the control group. It means there is herb-drug interactions between ADI and DOX. ADI can change the pharmacokinetics of DOX in HCC rats.

To the best of our knowledge, the plasma protein binding rate of DOX is very low. Therefore, ADI is unlikely to change the plasma concentration of DOX and DOXol by competing with plasma protein binding. ADI alters DOX's drug metabolism enzymes and transporters is a possible cause. DOX is mainly metabolized in the liver and excreted in bile, 50% of which are parent drugs, and 23% are active metabolites such as DOXol [25]. DOX can be converted into a semiquinone structure through single-electron reduction, and it can also form DOXol through C-13 hydroxylation in the cytoplasm by carbonyl reductase 1 (CBR1), which is generally expressed in liver, heart and other tissues [26]. Various transporters, particularly P-gp (ABCB1, MDR1) and ABCC1 (MRP1), are thought to play a role in resistance to DOX [2]. Generally, increased expression of P-gp results in increased DOX efflux and a number of studies on DOX resistance have shown that resistance can be overcome via inhibition of P-gp [27–29]. The import transporter SLC22A16 has also been shown to be involved in intracellular transport of DOX [30].

In our previous study, ADI also reduced mRNA levels and enzymatic activity of glutathione transferases (GSTs), and decreased protein expression of GST- $\pi$  in the livers of HCC rats [19]. High expression of GST- $\pi$  is known to accelerate the transformation and metabolism of anti-tumor drugs, shorten the duration of effective drug concentrations in cells and rapidly reduce the accumulation of drugs in target sites, thus reducing efficacy. GSTs are considered to be potential targets to overcome chemoresistance in solid tumors [31], and reduction of GSTs activity may be the one of underlying mechanisms for the synergistic effect of ADI. Inhibition of GSTs activity cannot, however, explain why administration of ADI leads to elevated levels of DOX and DOXol, since GSTs are not involved in DOX metabolism. In summary, to explain why ADI changed pharmacokinetics of DOX, more experiments with rigorous design are needed.

DOX is an effective chemotherapeutic drug. DOXol is the most important component of DOX-induced cardiotoxicity. Hence, increased blood concentrations of DOX and DOXol, in addition to implying that it may increase the therapeutic effect of DOX and may lead to stronger toxic and side effects. However, many studies have shown that the related ingredients of *Astragalus*, *A. senticosus*, *Ginseng* can play a synergistic effect, protect the heart, and reduce the toxic and side effects of chemotherapy drugs, such as ginsenoside Rg1 [32], ginsenoside Rg3 [33–35], astragalus polysaccharide [36–37], acanthopanax senticosides B [38]. Therefore, whether the combination of ADI and DOX can enhance the efficacy and reduce the myocardial toxicity of DOX requires more experiments to verify.

## 5. Conclusions

In this study, an accurate and validated UPLC-MS/MS method was developed to determine DOX and DOXol concentrations in rat plasma and then used to investigate DOX pharmacokinetics. Using this method, we identified potential herb-drug interactions between ADI and DOX. The AUCs of DOX and DOXol in rats pretreated with ADI were 3.79-fold and 2.92-fold higher, respectively, than AUCs in the control group. Further studies are needed to better understand the synergistic effect of ADI and DOX. Since both DOX and DOXol are implicated in the cardiotoxicity, in future studies we will investigate the cardiotoxicity of DOX and the distribution of DOX and DOXol in the heart and tumor tissue when DOX is co-administered with ADI.

# Abbreviations

## **ADI**

Aidi Injection

## **DOX**

Doxorubicin

## **DOXol**

Doxorubicinol

## **UPLC-MS/MS**

Ultra-performance Liquid Chromatography-Tandem Mass Spectrometry

## **DEN**

Diethylnitrosamine

## **IS**

Internal Standard

## **AUC**

The plasma drug concentration-time curve

## $t_{1/2\alpha}$

The half-life of distribution

## $V_1$

The apparent volume of distribution in the central compartment

## **CL**

The clearance

## $t_{1/2\beta}$

The elimination half-life

## $K_{10}$

The elimination rate constant of drug from compartment 1

## $K_{12}$

The rate constant for movement of drug from compartment 1 to compartment 2

## $K_{21}$

The rate constant for movement of drug from compartment 2 to compartment 1

## $MRT_{0-t}$

The mean residence time

## $t_{1/2z}$

The elimination half-life time

## $C_{max}$

The peak concentration

# Declarations

## Ethics approval and consent to participate

In vivo experiments were performed in accordance with international guidelines and experimental procedures performed with due approval from the Ethical Committee on Animal Studies of Guizhou Medical University (Approval number 1801207).

### **Consent for publication**

Not applicable.

### **Availability of data and materials**

The datasets used and/or analyzed during the current study are available from the corresponding author on reasonable request.

### **Competing of interests**

The authors declare that they have no competing interests.

### **Funding**

This work was financially supported by the National Natural Science Foundation of China (No. 81603189, No. 81860718), the Science and Technology Department of Guizhou Province ([2015]7361, [2017]5718), the Team Project of Guizhou Provincial Science and Technology Department ([2016]5613\5677), the Central Guidance for Local Science and Technology Projects ([2018]4006). These entities had no role in the design of the studies or the collection, analysis, or interpretation of data or in writing the manuscript.

### **Authors' contributions**

YL and TL designed research; YL, JP, SZ, CL, JS, YTL, SC, JH, CC, YW, YJL, TL performed research and analyzed the data; YL and TL wrote the paper. All authors read and approved the final manuscript.

### **Acknowledgements**

Not applicable.

## **References**

1. Omata M, Cheng AL, Kokudo N, Kudo M, Lee JM, Jia J, Tateishi R, Han KH, Chawla YK, Shiina S, Jafri W, Payawal DA, Ohki T, Ogasawara S, Chen PJ, Lesmana CRA, Lesmana LA, Gani RA, Obi S, Dokmeci AK, Sarin SK. Asia-Pacific clinical practice guidelines on the management of hepatocellular carcinoma: a 2017 update. *Hepatol Int.* 2017;11(4):317–70.
2. Cox J, Weinman S. Mechanisms of doxorubicin resistance in hepatocellular carcinoma. *Hepat Oncol.* 2016;3(1):57–9.
3. Thorn CF, Oshiro C, Marsh S, Hernandez-Boussard T, McLeod H, Klein TE, Altman RB. Doxorubicin pathways: pharmacodynamics and adverse effects. *Pharmacogenet Genomics.* 2011;21(7):440–6.

4. Xiao Z, Wang C, Li L, Tang X, Li N, Li J, Chen L, Gong Q, Tang F, Feng J, Li X. Clinical Efficacy and Safety of Aidi Injection Plus Docetaxel-Based Chemotherapy in Advanced Nonsmall Cell Lung Cancer: A Meta-Analysis of 36 Randomized Controlled Trials. *Evid Based Complement Alternat Med*. 2018;2018:7918258.
5. Xie G, Cui Z, Peng K, Zhou X, Xia Q, Xu D. Aidi Injection, a Traditional Chinese Medicine Injection, Could Be Used as an Adjuvant Drug to Improve Quality of Life of Cancer Patients Receiving Chemotherapy: A Propensity Score Matching Analysis. *Integr Cancer Ther*. 2019;18:1534735418810799.
6. Xiao Z, Wang C, Zhou M, Hu S, Jiang Y, Huang X, Li N, Feng J, Tang F, Chen X, Ding J, Chen L, Wang Y, Li X. Clinical efficacy and safety of Aidi injection plus paclitaxel-based chemotherapy for advanced non-small cell lung cancer: A meta-analysis of 31 randomized controlled trials following the PRISMA guidelines. *J Ethnopharmacol*. 2019;228:110–22.
7. Xie G, Cui Z, Peng K, Zhou X, Xia Q, Xu D. Aidi Injection, a Traditional Chinese Medicine Injection, Could Be Used as an Adjuvant Drug to Improve Quality of Life of Cancer Patients Receiving Chemotherapy: A Propensity Score Matching Analysis. *Integr Cancer Ther*. 2019;18:1534735418810799.
8. Liu D, Chen Z. The effects of cantharidin and cantharidin derivatives on tumour cells. *Anticancer Agents Med Chem*. 2009;9(4):392–6.
9. Han W, Wang S, Liang R, Wang L, Chen M, Li H, Wang Y. Non-ionic surfactant vesicles simultaneously enhance antitumor activity and reduce the toxicity of cantharidin. *Int J Nanomedicine*. 2013;8:2187–96.
10. Kim JA, Kim Y, Kwon BM, Han DC. The natural compound cantharidin induces cancer cell death through inhibition of heat shock protein 70 (HSP70) and Bcl-2-associated athanogene domain 3 (BAG3) expression by blocking heat shock factor 1 (HSF1) binding to promoters. *J Biol Chem*. 2013;288(40):28713–26.
11. Zhang W, Ma YZ, Song L, Wang CH, Qi TG, Shao GR. Effect of cantharidins in chemotherapy for hepatoma: A retrospective cohort study. *Am J Chin Med*. 2014;42(3):561–7.
12. Zhang YM, Liu YQ, Liu D, Zhang L, Qin J, Zhang Z, Su Y, Yan C, Luo YL, Li J, Xie X, Guan Q. The Effects of Astragalus Polysaccharide on Bone Marrow-Derived Mesenchymal Stem Cell Proliferation and Morphology Induced by A549 Lung Cancer Cells. *Med Sci Monit*. 2019;25:4110–21.
13. Zheng Y, Ren W, Zhang L, Zhang Y, Liu D, Liu Y. A Review of the Pharmacological Action of Astragalus Polysaccharide. *Front Pharmacol*. 2020;11:349.
14. Kondeva-Burdina M, Shkondrov A, Simeonova R, Vitcheva V, Krasteva I, Ionkova I. In vitro/in vivo antioxidant and hepatoprotective potential of defatted extract and flavonoids isolated from *Astragalus spruneri* Boiss. (Fabaceae). *Food Chem Toxicol*. 2018;111:631–40.
15. Li LK, Kuang WJ, Huang YF, Xie HH, Chen G, Zhou QC, Wang BR, Wan LH. Anti-tumor effects of Astragalus on hepatocellular carcinoma in vivo. *Indian J Pharmacol*. 2012;44(1):78–81.

16. Yoon TJ, Yoo YC, Lee SW, Shin KS, Choi WH, Hwang SH, Ha ES, Jo SK, Kim SH, Park WM. Anti-metastatic activity of *Acanthopanax senticosus* extract and its possible immunological mechanism of action. *J Ethnopharmacol.* 2004;93(2–3):247–53.
17. Yang X, Zou J, Cai H, Huang X, Yang X, Guo D, Cao Y. Ginsenoside Rg3 inhibits colorectal tumor growth via down-regulation of C/EBP $\beta$ /NF- $\kappa$ B signaling. *Biomed Pharmacother.* 2017;96:1240–5.
18. Dai G, Sun B, Gong T, Pan Z, Meng Q, Ju W. Ginsenoside Rb2 inhibits epithelial-mesenchymal transition of colorectal cancer cells by suppressing TGF- $\beta$ /Smad signaling. *Phytomedicine.* 2019;56:126–35.
19. Lu Y, Pan J, Yang ST, Wu Q, Liu CH, Li YJ, Liu T. Effect of Aidi injection on glutathione-S-transferase of diethylnitrosamine-induced hepatocellular carcinoma model rats. *Chin Pharma Bull.* 2018;34(8):1170–4.
20. Pan J, Lu Y, Zhang S, Li YT, Sun J, Liu CH, Gong ZP, Huang J, Cao C, Wang YL, Li YJ, Liu T. Differential changes in the pharmacokinetics of doxorubicin in diethylnitrosamine-induced hepatocarcinoma model rats [published online ahead of print, 2020 May 13]. *Xenobiotica.* 2020;1–7. doi:10.1080/00498254.2020.1765049.
21. Lu Y, Pan J, Yang ST, Liu CH, Li YJ, Liu T. Effect of Aidi injection on in vivo pharmacokinetics of doxorubicin in Sprague-Dawley rats by UPLC-MS method. *Chin Pharma Bull.* 2018;34(3):423–7.
22. Gomes AS, Monteleone PA, Sayre JW, Finn RS, Sadeghi S, Tong MJ, Britten CD, Busuttill RW. Comparison of triple-drug transcatheter arterial chemoembolization (TACE) with single-drug TACE using doxorubicin-eluting beads: Long-term survival in 313 patients. *AJR Am J Roentgenol.* 2017;209(4):722–32.
23. Sun JH, Zhou GH, Zhang YL, Nie CH, Zhou TY, Ai J, Zhu TY, Wang WL, Zheng SS. Chemoembolization of liver cancer with drug-loading microsphere 50–100  $\mu$ m. *Oncotarget.* 2017;8(3):5392–9.
24. Dai Y, Gao S, Liu X, Gao Q, Zhang L, Fan X, Zhu J. Effect of Aidi injection plus TACE on hepatocellular carcinoma: A meta-analysis of randomized controlled trials. *Evid. Based Complement. Alternat. Med.* 2018, 9196409.
25. Lal S, Mahajan A, Chen WN, Chowbay B. Pharmacogenetics of target genes across doxorubicin disposition pathway: a review. *Curr Drug Metab.* 2010;11:115–28.
26. Bains OS, Karkling MJ, Grigliatti TA, Reid RE, Riggs KW. Two nonsynonymous single nucleotide polymorphisms of human carbonyl reductase 1 demonstrate reduced in vitro metabolism of daunorubicin and doxorubicin. *Drug Metab Dispos.* 2009;37:1107–14.
27. Chen T, Wang C, Liu Q, Meng Q, Sun H, Huo X, Sun P, Peng J, Liu Z, Yang X, Liu K. Dasatinib reverses the multidrug resistance of breast cancer MCF-7 cells to doxorubicin by downregulating P-gp expression via inhibiting the activation of ERK signaling pathway. *Cancer Biol Ther.* 2015;16(1):106–14.
28. Zhao YY, Yu L, Liu BL, He XJ, Zhang BY. Downregulation of P-gp, Ras and p-ERK1/2 contributes to the arsenic trioxide-induced reduction in drug resistance towards doxorubicin in gastric cancer cell

- lines. *Mol Med Rep.* 2015;12(5):7335–43.
29. Nanayakkara AK, Follit CA, Chen G, Williams NS, Vogel PD, Wise JG. Targeted inhibitors of P-glycoprotein increase chemotherapeutic-induced mortality of multidrug resistant tumor cells. *Sci Rep.* 2018;8(1):967.
30. Lal S, Wong ZW, Jada SR, Xiang X, Chen Shu X, Ang PC, Figg WD, Lee EJ, Chowbay B. Novel SLC22A16 polymorphisms and influence on doxorubicin pharmacokinetics in Asian breast cancer patients. *Pharmacogenomics.* 2007;8(6):567–75.
31. Pljesa-Ercegovac M, Savic-Radojevic A, Matic M, Coric V, Djukic T, Radic T, Simic T. Glutathione transferases: potential targets to overcome chemoresistance in solid tumors. *Int J Mol Sci.* 2018;19(12):3785.
32. Zhu C, Wang Y, Liu H, Mu H, Lu Y, Zhang J, Huang J. Oral administration of Ginsenoside Rg1 prevents cardiac toxicity induced by doxorubicin in mice through anti-apoptosis. *Oncotarget.* 2017;8(48):83792–801.
33. Wang X, Chen L, Wang T, Jiang X, Zhang H, Li P, Lv B, Gao X. Ginsenoside Rg3 antagonizes adriamycin-induced cardiotoxicity by improving endothelial dysfunction from oxidative stress via upregulating the Nrf2-ARE pathway through the activation of akt. *Phytomedicine.* 2015;22(10):875–84.
34. Zhou B, Yan Z, Liu R, Shi P, Qian S, Qu X, Zhu L, Zhang W, Wang J. Prospective study of transcatheter arterial chemoembolization (TACE) with ginsenoside Rg3 versus TACE alone for the treatment of patients with advanced hepatocellular carcinoma. *Radiology.* 2016;280:630–9.
35. Li L, Ni J, Li M, Chen J, Han L, Zhu Y, Kong D, Mao J, Wang Y, Zhang B, Zhu M, Gao X, Fan G. Ginsenoside Rg3 micelles mitigate doxorubicin-induced cardiotoxicity and enhance its anticancer efficacy. *Drug Deliv.* 2017;24(1):1617–30.
36. Cao Y, Ruan Y, Shen T, Huang X, Li M, Yu W, Zhu Y, Man Y, Wang S, Li J. Astragalus polysaccharide suppresses doxorubicin-induced cardiotoxicity by regulating the PI3k/Akt and p38MAPK pathways. *Oxid Med Cell Longev.* 2014;2014:674219.
37. Cao Y, Shen T, Huang X, Lin Y, Chen B, Pang J, Li G, Wang Q, Zohrabian S, Duan C, Ruan Y, Man Y, Wang S, Li J. Astragalus polysaccharide restores autophagic flux and improves cardiomyocyte function in doxorubicin-induced cardiotoxicity. *Oncotarget.* 2017;8(3):4837–48.
38. Liang Q, Yu X, Qu S, Xu H, Sui D. *Acanthopanax senticosides* B ameliorates oxidative damage induced by hydrogen peroxide in cultured neonatal rat cardiomyocytes. *Eur J Pharmacol.* 2010;627(1):209–15.

## Tables

Table 1

Pharmacokinetic parameters of DOX in control and ADI groups after single intravenous administration of DOX (7 mg/kg) ( $\bar{x} \pm SD$ , n = 6)

Parameters	Control	ADI
$t_{1/2\alpha}$ (h)	0.074 ± 0.005	0.089 ± 0.017**
$t_{1/2\beta}$ (h)	2.734 ± 1.385	2.638 ± 1.108
$V_1$ (L/kg)	0.099 ± 0.026	0.028 ± 0.011**
CL (L/h/kg)	0.37 ± 0.15	0.099 ± 0.048*
$AUC_{0-t}$ (mg/L*h)	20.21 ± 11.22	76.50 ± 34.89**
$K_{10}$ (1/h)	3.91 ± 1.67	3.68 ± 1.69
$K_{12}$ (1/h)	5.26 ± 2.05	4.27 ± 0.73
$K_{21}$ (1/h)	0.77 ± 0.49	0.65 ± 0.48
Data are presented as mean ± SD (n = 6). *P < 0.05, **P < 0.01 versus control group.		
$t_{1/2\alpha}$ , half-life of distribution; $t_{1/2\beta}$ , half-life of elimination; $V_1$ , apparent volume of distribution in central compartment; CL, clearance; $AUC_{0-t}$ , area under plasma drug concentration-time curve; $K_{10}$ , elimination rate constant of drug from compartment 1; $K_{12}$ , rate constant for movement of drug from compartment 1 to compartment 2; $K_{21}$ , rate constant for movement of drug from compartment 2 to compartment 1.		

Table 2

Pharmacokinetic parameters of DOXol in control and ADI groups after single intravenous administration of DOX (7 mg/kg) ( $\bar{x} \pm SD$ , n = 6)

Parameters	Control	ADI
AUC <sub>0-t</sub> (mg/L*h)	5.62 ± 2.23	16.41 ± 2.91**
MRT <sub>0-t</sub> (h)	2.40 ± 0.32	5.33 ± 1.31**
t <sub>1/2z</sub> (h)	2.09 ± 0.98	4.99 ± 0.95**
T <sub>max</sub> (h)	0.33 ± 0.001	0.33 ± 0.001
CLz/F (L/h/kg)	1.33 ± 0.57	0.43 ± 0.08
Vz/F (L/kg)	4.43 ± 3.86	3.13 ± 0.98
C <sub>max</sub> (mg/L)	2.41 ± 1.04	8.34 ± 3.90**
Data are presented as mean ± SD (n = 6). **P < 0.01 versus control group.		
AUC <sub>0-t</sub> , area under plasma drug concentration-time curve; MRT <sub>0-t</sub> , mean residence time; t <sub>1/2z</sub> , half-life of elimination; T <sub>max</sub> , peak time; CLz, clearance; Vz, apparent volume of distribution; C <sub>max</sub> , maximum (peak) plasma drug concentration.		

## Figures

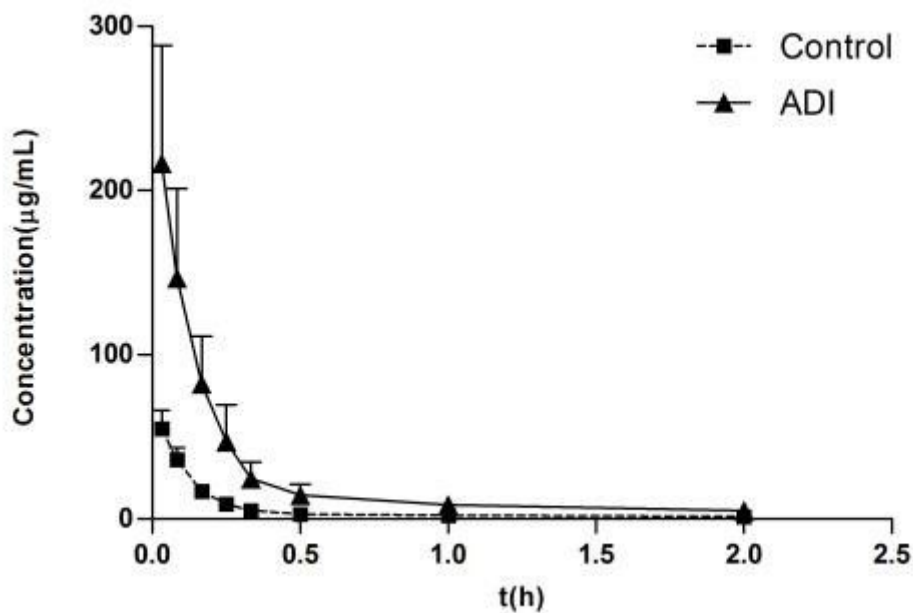


Figure 1

Plasma concentration-time profiles (Mean  $\pm$  SD, n = 6) of DOX in control and ADI groups.

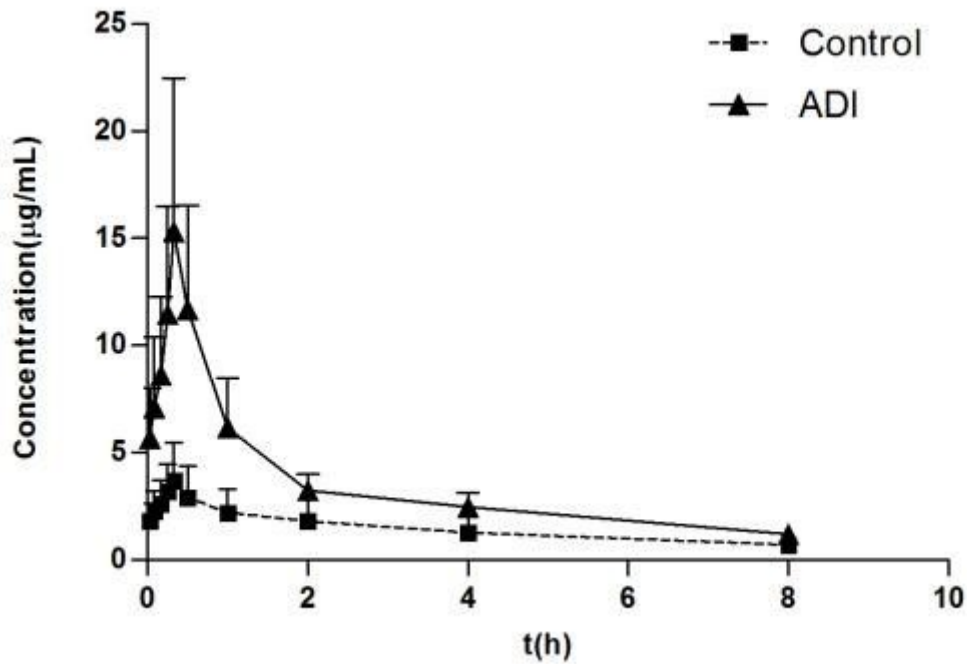


Figure 2

Plasma concentration-time profiles (Mean  $\pm$  SD, n = 6) of DOXol in control and ADI groups.

## Supplementary Files

This is a list of supplementary files associated with this preprint. Click to download.

- [NC3RsARRIVEGuidelinesChecklist.docx](#)